Modelling Simul. Mater. Sci. Eng. 3 (1995) 615–627. Printed in the UK

Molecular dynamics determination of defect energetics in β-SiC using three representative empirical potentials

Hanchen Huang†§, Nasr M Ghoniem†, Jimmy K Wong† and Michael I Baskes‡

† Mechanical Aerospace and Nuclear Engineering Department, University of California, Los Angeles, CA 90024, USA

‡ Sandia National Laboratories, Livermore, CA 94551, USA

Received 12 January 1995, accepted for publication 25 April 1995

Abstract. The determination of formation and migration energies of point and clustered defects in SiC is of critical importance to a proper understanding of atomic phenomena in a wide range of applications. We present here calculations of formation and migration energies of a number of point and clustered defect configurations. A newly developed set of parameters for the modified embedded-atom method (MEAM) is presented. Detailed molecular dynamics calculations of defect energetics using three representative potentials, namely the Pearson potential, the Tersoff potential and the MEAM, have been performed. Results of the calculations are compared to first-principles calculations and to available experimental data. The results are analysed in terms of developing a consistent empirical interatomic potential and are used to discuss various atomic migration processes.

1. Introduction

Silicon carbide (SiC) has been proposed as a candidate structural material for fusion reactor components [1, 2] which face intensive neutron irradiation damage [3]. Evolution of defects so produced determines many of the macroscopic properties of structural components. Determination of defect energetics which dominate defect evolution processes is therefore crucial to an understanding of the response of SiC to radiation damage. It is also considered for application as a high-temperature superconducting material. Carrier behaviour in such applications will be strongly dependent on point and clustered defects. A number of methods are available for studying defect energetics: experimental measurements [4, 5], first-principles calculations [6, 7], and computer simulations with empirical potentials (see, e.g., [8]). Experimental results are affected by many uncertain factors, and their interpretation is usually not unique. First-principles calculations are quite accurate but require very intensive computational efforts. Molecular dynamics (MD) simulations using empirical potentials are commonly used to study defect energetics with reasonable computational demands.

Empirical pair potentials have been successfully applied to calculations of some defect energetics in metals but have failed in describing covalent systems. There are quite a few empirical potentials proposed to describe many-body effects that are very important in covalent materials. This paper investigates defect energetics in SiC using three representative potentials: the Pearsaon potential, the modified embedded-atom method (MEAM) and the

§ Current address: Lawrence Livermore National Laboratory, L-268 PO Box 808, Livermore, CA 94550, USA

0965-0393/95/050615+13$19.50

Tersoff potential. The formation energies and migration energies of point defects, and antisite defect formation energies are calculated. Possible defect migration mechanisms are also investigated. The three representative potentials will be described and compared in more detail in section 2. The calculated results, available experimental data and first-principles calculations are summarized in section 3. A summary of our results and conclusions is finally presented in section 4.

2. Empirical potentials for β-SiC

Several empirical interatomic potentials exist for various materials, which can be classified into three categories:

(1) potentials developed following the Born–Openheimer expansion;
(2) potentials modelling local environment using electron distributions;
(3) potentials introducing local environment effects into pair potentials.

The three categories are represented by the Pearson potential, the MEAM and the Tersoff potential, respectively.

2.1. The Pearson potential

Pair potentials (Lennard-Jones [9], Morse [10], etc) have been successfully used in studying defects in metals and are capable of explaining some properties of close-packed structures that are common for metals. More open structures in semiconductors are a challenge for pair potentials. To account for many-body interactions, Born and Oppenheimer [11] proposed a general form for the interatomic potential, given by

$$\Phi_i(r_1, r_2, \ldots, r_n) = \frac{1}{2!}\sum_{j\neq i} V^{(2)}(r_{ij}) + \frac{1}{3!}\sum_{k\neq}\sum_{j\neq i} V^{(3)}(r_{ij}, r_{ik}, r_{jk}) + \cdots + \frac{1}{n!}\sum_{q\neq}\cdots\sum_{m\neq}\cdots\sum_{j\neq i} V^{(n)}(r_{ij}, \ldots, r_{iq}, \ldots, r_{mq}). \tag{1}$$

Environmental effects are included in the many-body interactions. To make this many-body potential practical in its applications, Pearson *et al* [12] truncated the expansion at the three-body level. For SiC, they combined the Lennard-Jones (6–12) two-body potential [9] and Axilrod–Teller [13] three-body potential in the form

$$V^{(2)}(r_{ij}) = \frac{\varepsilon}{m-n}\left[n\left(\frac{R_0}{r_{ij}}\right)^m - m\left(\frac{R_0}{r_{ij}}\right)^n\right] \tag{2}$$

$$V^{(3)}(r_{ij}, r_{ik}, r_{jk}) = Z\left[\frac{1+3\cos\theta_{ij}\cos\theta_{ik}\cos\theta_{jk}}{(r_{ij}r_{ik}r_{jk})^3}\right] \tag{3}$$

where the energy parameters ε and Z and the two-body structure parameter R_0 were adjusted to fit experimental data (sublimation energies and bond length) for bulk solid and atomic clusters for silicon element, carbon element and their compound. The three-body potential is a simple form which favours open structures. A modification was made by Huang and Ghoniem [8] to fit the sublimation energy exactly, and the modified potential is used in this paper.

The Stillinger–Weber [14] potential, which is similar to the Pearson potential, is another example of this type of potential. The Pearson potential has proven to be successful in some applications [8, 15–17]. Unfortunately, it fails in other cases where the system is far from

equilibrium configurations [18]. The Pearson potential uses 12 parameters. Two of them (m and n) are chosen by using the 6–12 Lennard-Jones pair potential. The other ten parameters are fitted to 16 experimental measurements of bond length and sublimation energies of several clusters and solids.

2.2. *The modified embedded-atom method*

The embedded atom method (EAM) was originally developed by Daw and Baskes [19, 20]. In this method, the potential energy of an atom in a crystal is divided into two parts:

(1) two-body core-core interactions with lattice atoms;
(2) energy needed to embed the atom into the background electron sea of the lattice.

Improvements and applications are being pursued at Sandia National Laboratories [21–30], University of Virginia [31–34], and other institutions [35–37]. The EAM was first developed on the basis of central pair potentials and spherically averaged electron densities. It was then modified to utilize angle-dependent electron densities in order to model covalent structures [22, 25, 29, 30].

The total configuration energy of a crystal is written as the sum of direct contributions from all atoms and is given by

$$E = \sum_i \left\{ F_i(\bar{\rho}_i) + \tfrac{1}{2} \sum_{j \neq i} \phi_{ij}(R_{ij}) \right\}. \tag{4}$$

In equation (4), the first term corresponds to an environment-dependent energy of embedding an atom, while the second term is the conventional pair potential. The embedding energy is assumed to be represented by

$$F_i(\bar{\rho}_i) = A_i E_i^0 \bar{\rho}_i \ln \bar{\rho}_i \tag{5}$$

where $\bar{\rho}_i$ is the background electron density at atom i, E_i^0 is the sublimation energy of atom i in the reference structure (diamond cubic) and A_i is a parameter.

The background electron density is given by

$$\bar{\rho}_i = \frac{\bar{\rho}_i^{(0)}}{\rho_i^0} \exp\left[-\tfrac{1}{2} \sum_{k=1}^{3} \left(\frac{\bar{\rho}_i^{(k)} t_i^{(k)}}{\bar{\rho}_i^{(0)}} \right)^2 \right] \tag{6}$$

where $\bar{\rho}_i^{(k)}$ are the partial electron densities, $t_i^{(k)}$ are the average weighting factors for the partial electron density and ρ_i^0 is the composition-dependent electron density scaling:

$$\rho_i^0 = \rho_{i0} Z_{i0} \exp\left(-\tfrac{1}{2} \sum_{k=1}^{3} \frac{s^{(k)} t_i^{(k)}}{z_{i0}^2} \right) \tag{7}$$

where Z_{i0} is the first-neighbour coordination of the reference system, $s^{(k)}$ are geometry factors and ρ_{i0} is a parameter.

The average weighting factors are given by

$$t_i^{(k)} = \sum_{j \neq i} t_{0,j}^{(k)} \rho_j^{(0)} S_{ji} \Big/ \sum_{j \neq i} \rho_j^{(0)} S_{ji} \tag{8}$$

where S_{ij} is the screening function and $t_{0,j}^{(k)}$ are parameters.

The partial electron densities are given by

$$\bar{\rho}_i^{(0)} = \sum_{j \neq i} \rho_j^{(0)} S_{ji} \tag{9}$$

$$(\bar{\rho}_i^{(1)})^2 = \sum_{\alpha=1}^{3} \left[\sum_{j \neq i} x_{ij}^{\alpha} \rho_j^{(1)} S_{ji} \right]^2 \tag{10}$$

$$(\bar{\rho}_i^{(2)})^2 = \sum_{\alpha,p=1}^{3} \left[\sum_{j \neq i} x_{ij}^{\alpha} x_{ij}^{p} \rho_j^{(2)} S_{ji} \right]^2 - \tfrac{1}{3} \left[\sum_{j \neq i} \rho_j^{(2)} S_{ji} \right]^2 \tag{11}$$

$$(\bar{\rho}_i^{(3)})^2 = \sum_{\alpha,p,q=1}^{3} \left[\sum_{j \neq i} x_{ij}^{\alpha} x_{ij}^{p} x_{ij}^{q} \rho_j^{(3)} S_{ji} \right]^2 \tag{12}$$

where α, p, $q = 1, 2, 3$ with the atomic electron densities

$$\rho_i^{(k)} = \rho_{i0} \exp\left[-\beta_i^{(k)} \left(\frac{R}{R_i^0} - 1 \right) \right] \text{with} k = 0, 1, 2, 3 \tag{13}$$

where R_i^0 is the nearest-neighbour distance in the reference structure and $\beta_i^{(k)}$ are parameters.

The scaled coordinates x_{ij}^m are given by

$$x_{ij}^1 = \frac{x_j - x_i}{r_{ij}} \qquad x_{ij}^2 = \frac{y_j - y_i}{r_{ij}} \qquad x_{ij}^3 = \frac{z_j - z_i}{r_{ij}} \tag{14}$$

with r_{ij} the distance between atoms i and j.

The screening function is given by $S_{ji} = \Pi_{k \neq i,j} S_{jki}$ and

$$S_{jki} = \begin{cases} 0 \\ \left(1 - \left(\dfrac{C_{\max} - C}{C_{\max} - C_{\min}} \right)^4 \right)^2 \\ 1 \end{cases} \quad \text{for} \begin{cases} C \leqslant C_{\min} \\ C_{\min} \leqslant C \leqslant C_{\max} \\ C \geqslant C_{\max} \end{cases} \tag{15}$$

where

$$C = 1 + 2 \frac{r_{jk}^2 r_{ji}^2 + r_{ki}^2 r_{ji}^2 - r_{ji}^4}{r_{ji}^4 - (r_{jk}^2 - r_{ki}^2)^2}.$$

$C_{\min}$ and $C_{\max}$ are parameters.

In averaging the weighting factors $t_i^{(k)}$, the effect of electrons from dissimilar atoms in a multicomponent system are considered. The screening function S_{ji} is introduced to account for relative contributions from atoms at different locations and can be regarded as a force cut-off technique.

The pair potential is derived from the universal equations of state [38, 39] as follows:

$$E_i^u(R) = -E_i^0 \left[1 + \alpha_i \left(\frac{R}{R_i^0} - 1 \right) \right] \exp\left[-\alpha_i \left(\frac{R}{R_i^0} - 1 \right) \right] \tag{16}$$

$$E_i(R) = \tfrac{1}{2} \{ F_i(\bar{\rho}_j) + F_j(\bar{\rho}_j) + Z_{ij0} \phi_{ij}(R) \} \tag{17}$$

and with screening effects it is given as

$$\phi_{ij}(R) = \frac{1}{Z_{ij0}} \{ 2E_i^u(R) - F_i(\bar{\rho}_j) - F_j(\bar{\rho}_i) \} S_{ji} \tag{18}$$

It is worthwhile mentioning that the pair potential is defined using the embedding function at a reference structure and that the $\bar{\rho}_i$ is calculated using equation (6) evaluated

Table 1. Parameters of the MEAM: N/A, not applicable.

Parameters	Si	C	Si–C
A	1	1	N/A
ρ_0	1.0	2.25	N/A
R^0 (Å)	2.3517	1.5446	1.8878
E^0 (eV)	4.63	7.37	6.433
α	4.87	4.38	4.37
$\beta^{(0)}$	4.8	4.1	N/A
$\beta^{(1)}$	4.8	4.2	N/A
$\beta^{(2)}$	4.8	5.0	N/A
$\beta^{(3)}$	4.8	3.0	N/A
$t_0^{(0)}$	1.0	1.0	N/A
$t_0^{(1)}$	3.3	5.0	N/A
$t_0^{(2)}$	5.105	9.34	N/A
$t_0^{(3)}$	−0.8	−1.00	N/A
$C_{\min}$	2.0	2.0	2.0
$C_{\max}$	2.8	2.8	4.0

Table 2. Geometry factors for a diamond cubic lattice.

$S^{(0)}$	$S^{(1)}$	$S^{(2)}$	$S^{(3)}$	Z_0
1	0	0	32/9	4

in the reference structure. For a more detailed explanation, readers are referred to [29, 40]. For single elements, the parameters are determined by fitting to the sublimation energy, the lattice constant, the bulk modulus, two shear constants, structure energy differences and the vacancy formation energy. The MEAM uses 14 parameters (excluding the geometry factors) to fit the properties of each element (Si or C). An additional six parameters are used to represent SiC. The relative magnitudes of ρ_{Si} and ρ_C, are determined by fitting to the vacancy formation energy of an atom pair in the diatomic system. Two parameters are used to define screening functions. The other three parameters are determiend by lattice constant, sublimation energy and bulk modulus of SiC. The calibration process has been described in [40]. The parameters of the MEAM for SiC are listed in table 1 and the geometry factors in table 2.

2.3. The Tersoff potential

Tersoff extended the conventional pair potential to describe many-body effects by assuming that the pair potential coefficients depend on the local environment [41, 42]. The computational time of MD simulation with pair-like potentials is thus dramatically reduced compared to that employing three-body potentials. The potential is composed of two parts for repulsive and attractive interactions. The local environment is described by a measure of bond order in the attractive interaction. The bond strength is explicitly related to the coordination number, which renders close-pcked or open structures a natural result of competition between bond strength and the coordination number. The potential, after being successfully used for pure elements [43, 44], was extended to multicomponent systems by interpolation [45–47]. Only one parameter was introduced to scale the relative bond order of the elements involved. The general potential function for multicomponent systems can

be written as

$$E = \frac{1}{2}\sum_{i,j\neq i} f_c(r_{ij})[A_{ij}\exp(-\lambda_1 r_{ij}) - B_{ij}b_{ij}\exp(-\lambda_2 r_{ij})] \tag{19}$$

with bond order described by

$$b_{ij} = \chi_{ij}(1+\beta_i^{n_i}\zeta_{ij}^{n_i})^{-1/2n_i} \tag{20}$$

$$\zeta_{ij} = \sum_{k\neq i,j} f_c(r_{ik})g(\theta_{ijk}) \tag{21}$$

$$g(\theta_{ijk}) = 1 + \frac{c_i^2}{d_i^2} - \frac{c_i^2}{d_i^2 + (h_i - \cos\theta_{ijk})} \tag{22}$$

where the cut-off function $f_c(r_{ij})$ is given by

$$f_c(r_{ij}) = \begin{cases} 1 \\ \frac{1}{2} + \frac{1}{2}\cos\left(\dfrac{r_{ij}-R_{ij}}{S_{ij}-R_{ij}}\pi\right) \\ 0 \end{cases} \qquad \text{for} \begin{cases} r_{ij} < R_{ij} \\ R_{ij} < r_{ij} < S_{ij} \\ r_{ij} > S_{ij}. \end{cases} \tag{23}$$

Table 3. Parameters of the Tersoff potential.

Parameter	Carbon	Silicon
A (eV)	1.5448×10^3	1.8308×10^3
B (eV)	3.8963×10^2	4.7118×10^2
λ (Å^{-1})	3.4653	2.4799
μ (Å^{-1})	2.3064	1.7322
β	4.1612×10^{-6}	1.1000×10^{-6}
n	9.9054×10^{-1}	7.8734×10^{-1}
c	1.9981×10^4	1.0039×10^5
d	7.0340	1.6217×10^1
h	-3.9953×10^{-1}	-5.9825×10^{-1}
R (Å)	1.8	2.7
S (Å)	2.1	3.0
	$\chi_{C-Si} = 1.0121$[a]	

[a] The original value from Tersoff was 1.0086, which gives 12.735 eV sublimation energy. To maje a consistent comparison of the potentials, we calibrate the χ_{C-Si} to be 1.0121 to fit 12.865 eV for the experimental sublimation energy, which is used in the other two potentials. The difference in the results caused by this modification is small (mostly 3–5%).

Parameters for multicomponent systems are related to those for single elements by arithmetic or geometric averages:

$$\lambda_{ij} = \frac{\lambda_i + \lambda_j}{2} \tag{24}$$

$$\mu_{ij} = \frac{\mu_i + \mu_j}{2} \tag{25}$$

$$A_{ij} = (A_i A_j)^{1/2} \tag{26}$$

$$B_{ij} = (B_i B_j)^{1/2} \tag{27}$$

$$R_{ij} = (R_i R_j)^{1/2} \tag{28}$$

$$S_{ij} = (S_i S_j)^{1/2}. \tag{29}$$

Parameters for single elements are determined by fitting to the sublimation energy, the lattice constant, the bulk modulus of the diamond structure, and the cohesive energies of other polytypes (dimer, SC and FCC) of the material. The single parameter χ_{ij} for each pair of dissimilar atoms is determined by fitting to the correct heat of formation. The parameters determined by Tersoff [47, 48] are listed in table 3. The Tersoff potential uses 11 parameters to fit the properties of each element (silicon or carbon). One additional parameter is used to fit the heat of formation for SiC. Two parameters are used to define the cut-off for each element, which are assumed to be unaffected in a compound.

2.4. *Features of empirical potentials*

Some common features are shared among the three potentials, while others diverge. Their main features are summarized in the following paragraphs.

The elastic constants (bulk moudulus K and shear modulus $\gamma' = (C_{11} - C_{12})/2$) of β-SiC are calculated using the three empirical potentials. In table 4, the results are compared to theoretical calculations for β-SiC [52], which was confirmed by experiments on 6H-SiC [53]. Predictions from both the MEAM and the Tersoff potential are in good agreement with the experimental data, while those from the Pearson potential are not.

Table 4. Elastic constants of β-SiC.

	Value (GPa)			
Constants	Pearson	MEAM	Tersoff	Experiments [52, 53]
K	1183	211	189	211
γ'	87	140	143	106

Development of all the three potentials considers the effects of the local environment (i.e. many-body interactions). The MEAM was developed on the basis of quantum-mechanical results, giving an angular dependence of spatial distribution of outer electrons. It is the electron distribution that determines the local environment. The Tersoff potential was developed on the physical basis that the bond order depends on the coordination number. A trade-off of these two factors results in either a close-packed or open structure. Angular dependence was introduced to account for the fact that the bond order is affected by the relative angles of neighbouring bonds. The Pearson potential, on the other hand, was obtained by truncating the Born–Oppenheimer expansion at the three-body level. All higher-order effecys (many-body interactions) are assumed to be either small or represented by the three-body interaction form.

The three potentials have quite different approaches to account for the fact that atoms far from a site have smaller contributions to it. The MEAM employed a screening function such that two atoms interact at all distances except when a third atom intervenes in (screens) the interaction. The Tersoff potential used a smooth cut-off function such that, as an atom is farther away from the site, its influence to the site becomes smaller. There is no explicit form of cut-off in the Pearson potential that makes it short ranged.

Screening by unlike atoms is taken into account in the MEAM by defining different unscreened configurations for a compound and elements. The Tersoff potential assumes that cut-off parameters (which correspond to unscreened and totally screened configurations) are the same for elements and a compound. The cut-off function determines the migration barrier by affecting the configurational energy at a saddle point. In this paper, the screening

(or cut-off) function in the MEAM is adjusted to give reasonable migration energies, while that in the Tersoff potential is used as it was.

In addition to prediction accuracy, one of the most important indices measuring the quality of an empirical potential is computational simplicity. In MD simulations, each step takes about 1.20×10^{-3} s/atom with the Pearson potential, 4.7×10^{-4} s/atom with the MEAM and 3.9×10^{-4} s/atom with the Tersoff potential (all are in CPU of CRAY-A at NERSC). The computational effort is therefore greatly reduced using the Tersoff potential or the MEAM, in comparison with the Pearson potential.

3. Results

In this section, we calculate various energies of defect formation and migration in β-SiC, using the three potentials presented in section 2. In a multicomponent system, the energy recovered when a single atom is placed on a crystal surface is ambiguous. Depending on the surface condition, the amount of the surface energy recovery could vary (see, e.g., [6, 7]). To avoid any confusion in defining defect energetics, an infinite vacuum rather than a real crystal is taken as a reference system. That is, to form a vacancy, an atom will be taken from the solid to a vacuum at infinity. Similarly, an interstitial is formed by taking an atom from infinity and putting it at an interstitial site. It is worthwhile to mention that defect migration energies are independent of the refernce system, whereas defect formation energies are dependent. We adjust the calculated values by 6.43 eV (one half of the pair sublimation energy) when we compare them with experimental data. In the case of a vacancy, this amount is subtracted from the calculated value, while it is added to the calculated value in the case of an interstitial.

A $2 \times 2 \times 2$ computational cell with periodic boundary conditions is used in the MD calculations. Energy minimization is done by using the conjugate-gradient method [54]. The cell volume is kept constant, while the total energy is not conserved. In the calculations of defect formation energies, the defected computational cell is set to relax fully. For the calculations of defect migration energies, on the other hand, the defect is fixed along one or two directions. Two corner atoms are also fixed to avoid movement of the computational cell as a whole. Other atoms are allowed to relax fully under these constraints. Size effects are investigated by employing a larger computational cell. It is found that the size effects do not give rise to errors of more than 0.01 eV. The migration paths are checked to be continuous in the three-dimensional space. Symmetry around a defect is slightly perturbed before relaxation to avoid possible configurations with zero forces and high configuration energies.

The results of our calculations are presented in table 5. All the energies presented are for fully relaxed configurations. The formation energies of vacancies, antisite defects and interstitials at TC (tetrahedral site surrounded by four carbon atoms) and TSi (tetrahedral site surrounded by four silicon atoms), and migration energies of vacancies and interstitials are calculated. H and B interstitial configurations are asymmetrical (net force is not zero) in SiC and are therefore unstable. Calculations of conventional vacancy migration using these empirical potentials show that the carbon vacancy migration energy is so high that carbon vacancies are not mobile below 1200 °C. Since appreciable vacancy clustering is observed in SiC above approximately 1000 °C [49], a conventional migration mechanism alone cannot therefore be responsible for atomic diffusion. When a migrating vacancy is assisted by an opposite type of vacancy, the migration energy is found to be reasonable. The two migration mechanisms of a silicon vacancy considered are shown in figure 1; those for a carbon vacancy are similar. Through the direct migration mechanism, a carbon vacancy, or

equivalently its nearest-neighbour carbon atom, jumps to one of its equivalent sites directly. In this process, it has to come close to several silicon atoms which are large in size. The migration path for the carbon atom is narrow, and the migration energy is high. Through the indirect migration mechanism, one silicon atom along the migration path is absent and more space is available for a carbon atom to migrate through. Due to the smaller size of carbon atoms, a silicon vacancy (or equivalently an atom) can migrate directly through a region surrounded by several carbon atoms. The indirect migration mechanism can be operative when vacancies are abundant, which is the case in irradiated samples. The antisite diffusion mechanism [51] could also be operative if sufficient antisite defects are introduced during sample processing. This mechanism is not fully investigated in this paper since antisite defects are unlikely to form under normal conditions (see the large formation energies in table 5).

An interstitial can directly migrate from one lower-energy T position to another neighbouring equivalent T position. Migration of interstitials by exchanging with neighbouring lattice atoms (knock-off mechanism) is found to experience a higher potential barrier than direct migration does. Migration of an interstitial assisted by another neighbouring interstitial is also investigated and is found to give high migration energies. The direct migration mechanism is therefore operative for interstitials in SiC. The direct migration mechanism for a silicon interstitial is shown in figure 2, while that for a carbon interstitial is similar. An interstitial jumps from the lowest-energy T position to a nearest-neighbouring T position which is the opposite type and then jumps to the next-nearest-neighbour T position which is equivalent.

Swelling experiments show that interstitial loops are formed even at room temperature, while vacancy clusters (cavities) are formed only above 1000 °C [49]. These indicate that at least one type of interstitial is mobile at room temperature, while vacancies start to migrate at 1000 °C. In other words, one type of interstitial must have a migration energy of about 1 eV and one type of the vacancy must have a migration energy of about 3 eV. With the MEAM, we can predict a reasonable carbon interstitial migration energy and vacancy migration energy. The vacancy migration energy predicted by the Tersoff potential is also within reasonable range, but the Tersoff potential does not give a very low interstitial migration energy due to its cut-off function.

Based on the MEAM, the activation energy of silicon self-diffusion (thermal diffusion through vacancy mechanism) is 10.73 eV, while that of carbon self-diffusion is 8.39 eV (the values are adjusted as mentioned at the beginning of this section). The results are in good agreement with experimental data, which are 9.50 eV and 8.70 eV for silicon and carbon, respectively [4–5]. Those using the Tersoff potential are 11.86 eV and 14.12 eV, respectively. The fact that migration and activation energies predicted by the Tersoff potential are not fully satisfactory can be accounted for by the screening function as discussed in section 2.

The first-principles calculation and the MD calculations using the MEAM and the Tersoff potential predict a large energy increase for forming a pair of antisite defects, which means that the β-SiC structure is stable against the formation of carbon and silicon clusters. Prediction from the Pearson potential is too small and is believed to be unreasonable.

All the calculations, including the first-principles calculations and the MD calculations using the three empirical potentials, show that the size effect is important. An interstitial is likely to take a TC site rather than a TSi site because TC is more spacious than TSi. Another example showing the size effect is the vacancy migration processes, during which the silicon vacancy can migrate easily through a group of carbon atoms while a carbon vacancy cannot migrate through a group of silicon atoms.

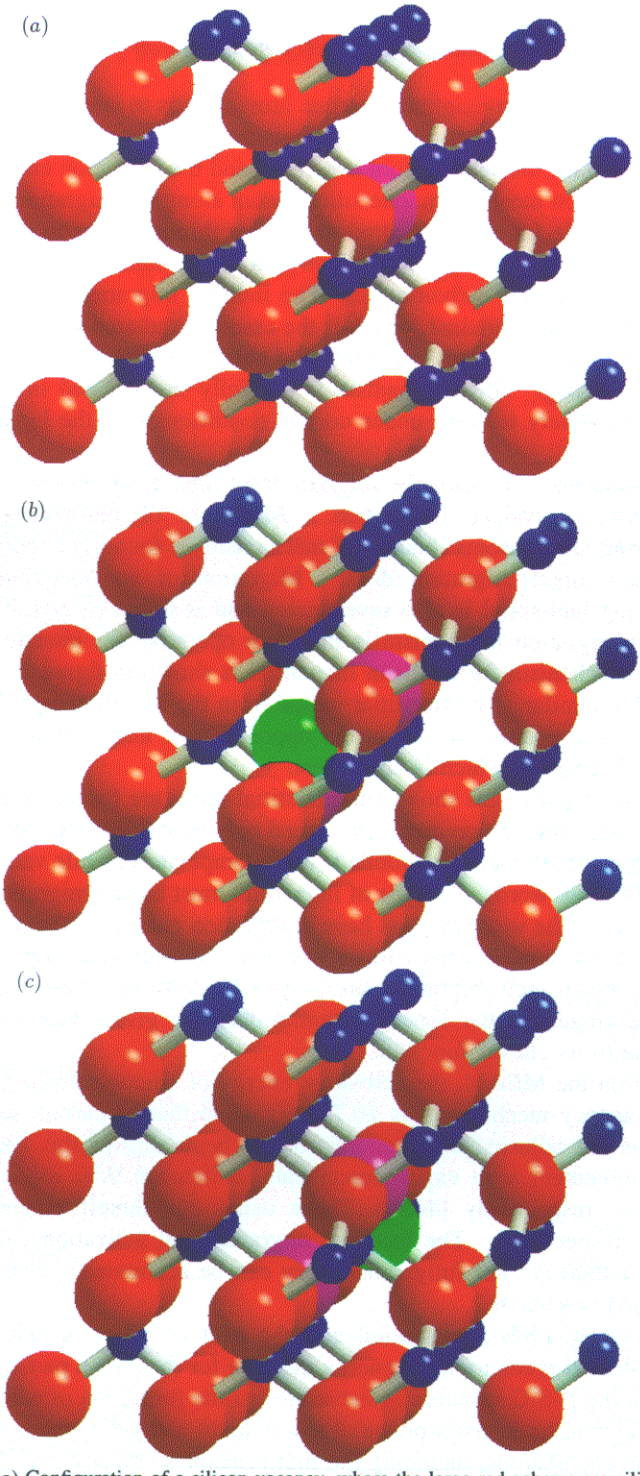

Figure 1. (*a*) Configuration of a silicon vacancy, where the large red spheres are silicon lattice atoms, the large magenta sphere is a silicon vacancy, and the small blue spheres are carbon lattice atoms. (*b*) Configuration of direct silicon vacancy migration, where the large red spheres are silicon lattice atoms, the large magenta spheres are silicon vacancies, the large green sphere is a silicon atom at a saddle point, and the small blue spheres are carbon lattice atoms. (*c*) Configuration of indirect silicon vacancy migration, where the large red spheres are silicon lattice atoms, the large magenta spheres are silicon vacancies, the large green sphere is a silicon atom at a saddle point, and the small blue spheres are carbon lattice atoms.

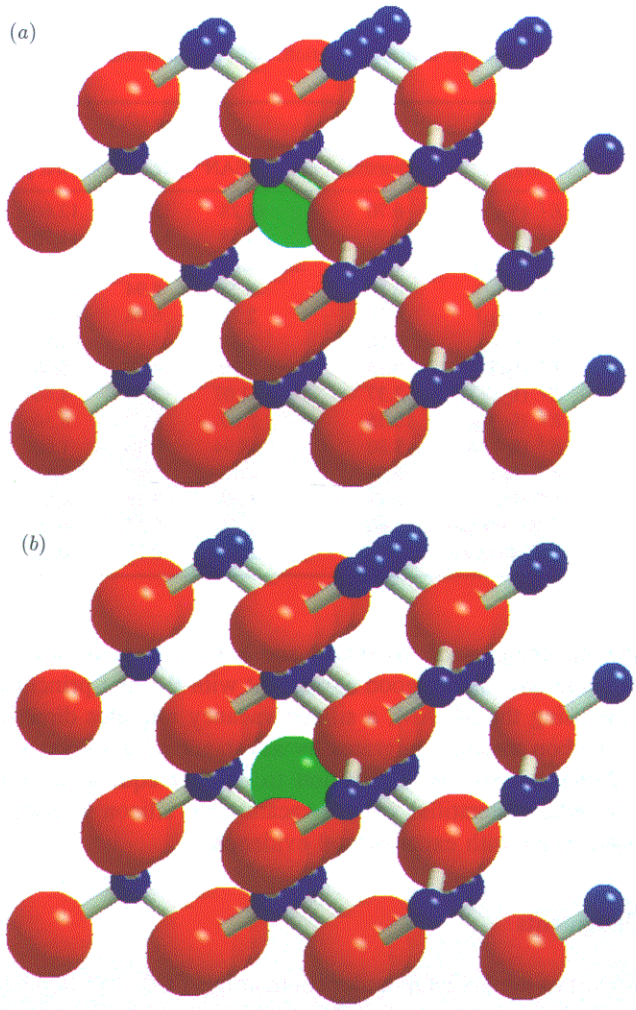

Figure 2. (*a*) Configuration of a silicon interstitial at TC (interstitial site), where the large red spheres are silicon lattice atoms, the large green sphere is a silicon interstitial, and the small blue spheres are carbon lattice atoms. (*b*) Configuration of a silicon interstitial at TSi (interstitial saddle point), where the large red spheres are silicon lattice atoms, the large green sphere is a silicon interstitial, and the small blue spheres are carbon lattice atoms.

4. Summary

The MEAM is calibrated for SiC and compared with the Tersoff potential and the Pearson potential. The formation energies predicted by using both the MEAM and the Tersoff potential are in good agreement with the first-principles calculations, with those from the Tersoff potential a little better. On the other hand, the MEAM does better in predicting migration energies. In essence, these two potentials are quite similar [50]. The Pearson potential does not even reproduce correct elastic constants, which are equilibrium properties. We recommend that the Pearson potential should be avoided, at least in studying defect configurations in bulk SiC. The first-principles calculation and our MD calculations using the MEAM and the Tersoff potential show that β-SiC is stable against antisite defect formation.

Table 5. Results of defect energetics of SiC: I, interstitial,; V, vacancy; m, migration; dm, direct migration; id, indirect migration; N/A, not applicable. The first-principles calculations are from [6, 7].

	Value (eV)			
Energy	Pearson *et al*	MEAN	Tersoff	First principles [6, 7]
E^f (V_{Si})	6.70	14.28	12.46	12.60
E^f (V_C)	5.26	9.58	11.61	11.70
E^{dm} (V_{Si})	7.39	2.88	5.83	N/A
E^{dm} (V_C)	6.10	5.24	8.94	N/A
E^{im} (V_{Si})	4.30	2.72	6.08	N/A
E^{im} (V_C)	0.50	2.61	3.48	N/A
E^f ($I_{Si}T_C$)	3.23	5.96	4.08	8.00
E^f (I_CT_C)	3.37	3.07	2.29	4.40
E^f ($I_{Si}T_{Si}$)	10.55	2.09	8.00	8.30
E^f (I_CT_{Si})	3.80	3.04	0.23	1.90
E^m (I_{Si})	6.04	4.12	3.95	N/A
E^m (I_C)	1.47	1.29	3.58	N/A
E(Si antisite)	3.66	7.21	5.55	6.40
E(C antisite)	3.33	2.17	0.61	0.20

The formation energies of vacancies and antisite defects based on the MEAM and the Tersoff potential are also in good agreement with the first-principles calculations. Based on calculations using the MEAM, a silicon vacancy migrates directly from one lattice site to another, a carbon vacancy migrates by assistance of a silicon vacancy, and an interstitial migrates directly from one T position to another equivalent T position. The migration energies of carbon interstitial, carbon vacancy and silicon vacancy based on the MEAM are in good agreement with experimental evidence.

Acknowledgments

Partial support of the US DOE under contract DE-FG03-91ER54115 with UCLA, and partial support of US DOE under contract DE-AC04-94AL85000 with Sandia National Laboratories are greatly appreciated. It is a great pleasure to thank Dr J Tersoff at IBM for providing us with updated potential parameters prior to publication. Thanks are also extended to Dr M Guinan, Professor R Johnson, and many other participants of the Santa Barbara Workshop on SiC (Summer 1993) for their stimulating comments on this topic. Dr T Diaz de la Rubia, Dr A Caro, Dr J Perlado and Dr M Guinan at LLNL are greatly acknowledged for providing us with their MD code employing the Tersoff potential. Discussions with Dr M Guinan on elastic moduli of SiC were also very valuable.

References

[1] Sharafat S, Wong C and Reis E 1991 *Fusion Technol.* **19** 901–7
[2] Trantina G 1979 *J. Nucl. Mater.* **85–6** 415–20
[3] Huang H and Ghoniem N 1993 *J. Nucl. Mater.* **199** 221–30
[4] Hon M and Davis R 1979 *J. Mater. Sci.* **14** 2411
[5] Hon M and Davis R 1980 *J. Mater. Sci.* **15** 2073
[6] Wang C, Bernholc J and Davis R 1988 *Phys. Rev.* B **38** 12752–5
[7] Bernholc J, Kajihara S, Wang C, Antonelli A and Davis R 1992 *Mater. Sci. Eng.* B **11** 265–72

[8] Huang H and Ghoniem N 1994 *J. Nucl. Mater.* **215** 148–153
[9] Lennard-Jones J 1939 *Interatomic Forces (Spec. Publ. VIII)* (Calcutta: Indian Association for the Cultivation of Science)
[10] Olander D 1976 *Fundamental Aspects of Nuclear Reactor Fuel Elements* (Washington, DC: Technical Information Center, Energy Research and Development Administration) ch 4
[11] Ziman J 1965 *Principles of the Theory of Solids* (Cambridge: Cambridge University Press) ch 6.10
[12] Pearson E, Takai T, Halicioglu T and Tiller W 1984 *J. Cryst. Growth* **70** 33–40
[13] Axilrod B and Teller E 1943 *J. Chem. Phys.* **11** 299–300
[14] Stillinger F and Weber T 1985 *Phys. Rev.* B **31** 5262–71
[15] Elazab A and Ghoniem N 1992 *J. Nucl. Mater.* **191–4** 1110–3
[16] Erkoc S, Halicioglu T and Tiller W 1992 *Surf. Sci.* **274** 359–62
[17] Balamane H, Halicioglu T and Tiller W 1992 *Phys. Rev.* B **46** 2250–79
[18] Biswas R and Hamann D 1985 *Phys. Rev. Lett.* **55** 2001–4
[19] Daw M and Baskes M 1983 *Phys. Rev. Lett.* **50** 1285–92
[20] Daw M and Baskes M 1984 *Phys. Rev.* B **29** 6443–53
[21] Foiles S, Baskes M and Daw M 1986 *Phys. Rev.* B **33** 7983–91
[22] Baskes M 1987 *Phys Rev. Lett.* **59** 2666–9
[23] Foiles S, Baskes M and Daw M 1988 *Mater. Res. Soc. Symp. Proc.* **122** 343–54
[24] Daw M 1989 *Phys. Rev.* B **39** 7441–52
[25] Baskes M, Nelson J and Wright A 1989 *Phys. Rev.* B **40** 6085–100
[26] Foiles S, Baskes M and Daw M 1989 *Mater. Sci. Forum* **37** 223–34
[27] Daw M 1989 *Atomic Simulation of Materials* ed V Vitek and D Srolovitz (New York: Plenum) pp 181–91
[28] Baskes M, Daw M and Foiles M 1989 *Mater. Res. Soc. Symp. Proc.* **141** 31–41
[29] Baskes M 1992 *Phys. Rev.* B **46** 2727
[30] Baskes M and Johnson R 1994 *Modeling Simulation Mater. Sci. Eng.* **2** 147–63
[31] Johnson R 1988 *Phys. Rev.* B **37** 3924
[32] Oh D and Johnson R 1988 *J. Mater. Res.* **3** 471
[33] Johnson R and Oh D 1989 *Mater. Res.* 4 1195
[34] Oh D and Johnson R 1989 *Mater Res. Soc. Symp. Proc.* **141** 31
[35] Voter A and Chen S-P 1987 *Mater. Res. Symp. Proc.* **82** 175
[36] Yoo M, Daw M and Baskes M 1989 *Atomic Simulation of Materials* ed V Vitek and Srolovitz (New York: Plenum) p 401
[37] Savino R, Rao S and Pasinot R 1987 *Mater. Res. Symp. Proc.* **141** 43
[38] Rose J. Smith J, Guinea F and Ferrante J 1984 *Phys. Rev.* B **29** 2963
[39] Banerjea A and Smith J 1988 *Phys. Rev.* B **37** 6632
[40] Baskes M 1994 *Computational Materials Modeling* ed A Noor and A Needleman (New York: ASME) p 23–35
[41] Tersoff J 1986 *Phys. Rev. Lett.* **56** 632–5
[42] Tersoff J 1988 *Phys. Rev.* B **37** 6991–7000
[43] Tersoff J 1988 *Phys. Rev. Lett.* **61** 2879–82
[44] Tersoff J 1988 *Phys. Rev.* B **38** 9902–5
[45] Kelires P and Tersoff J 1989 *Phys. Rev. Lett.* **63** 164–7
[46] Tersoff J 1990 *Phys. Rev. Lett.* **64** 1757–60
[47] Tersoff J 1989 *Phys. Rev.* B **39** 556–68
[48] Tersoff J 1995 *Phys. Rev.* B at press
[49] Miyazaki H, Suzuki T, Yano T and Iseki T 1992 *J. Nucl. Sci. Technol.* **29** 656–63
[50] Brenner D 1989 *Phys. Rev. Lett.* **63** 1022
[51] Birnie D III 1986 *J. Am. Ceram. Soc.* **69** C33–5
[52] Tolpygo K 1960 *Sov. Phys.–Solid State* **2** 2367–76
[53] Arlt G and Schodder G 1965 *J. Acoust. Soc. Am.* **37** 384–6
[54] Press W, Flannery B, Teukolsky S and Vetterling W 1992 *Numerical Recipes in Fortran* 2nd edn (Cambridge: Cambridge University Press) p 413